

# Dynamical processes in lipid membranes

Juan Pablo Guerrero Felipe\*, Egemen Yüzbaşı†, and Hitesh Patil‡

May 3, 2022

## Abstract

In this experiment we will examine features of the fluorophore probe by specifying the excitation and emission spectra of it. Further, we are going to analyze the dynamics of a lipid membrane at several temperatures with the help of steady-state and time resolved fluorescence measurements using DPH(Diphenylhexatriene) as a fluorophore. The measurements will be possible by measuring the anisotropy of the fluorescence. Under favor of highly hydrophobic behaviour of DMPC (diphenylhexatrien) some properties such as microviscosity order, van't Hoff enthalpy and cooperativity of the lipids' phase transition in lipid membranes can become more understandable. [1]

## 1 Theory and Concepts

### 1.1 Introduction of Fluorescence and Absorption Processes.

Once incident photons achieve any atom or molecule, it can excite electrons into upper energy levels, this process is called absorption (or excitation). The electrons, that were excited, can get a relaxation from the excited state to the ground state as a spontaneous emission, this process is called fluorescence. Absorption and fluorescence processes are radiative processes since the photons are scattered in an elastic process. However, it is just a small window of possible pathways for the electron relaxation. A more complete and detailed scheme of it is shown in the next diagram (Jablonski diagram).

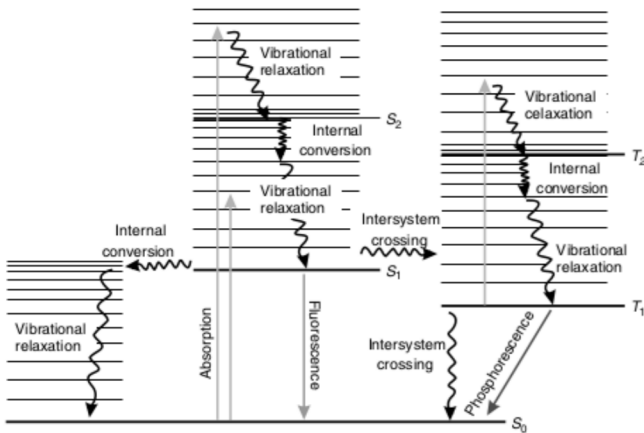


Figure 1: Jablonski diagram shows the processes that can occur upon excitation. First of all, electrons can come back to the initial ground state ( $S_0$ ) by emitting photons as a fluorescence signal. However there are other processes that can occur too. These processes are non-radiative and decrease the fluorescence amount of photons. Source [2]

Usually, these additional processes are inelastic processes, then electrons get a non-radiative relaxation. Examples of it are intersystem crossing, internal conversion, vibrational

relaxation... In particular vibrational relaxation ends up in the so called Stokes shift.

### 1.2 Stokes Shift

Once electrons are in an excited state, they can relax with a non-radiative process within the excited state, later on, fluorescence occurs. However, since electrons have experienced an additional process, they have lost some of its energy by a vibrational relaxation. Then, emitted photons have less energy than the original excitation. Energy related to these processes is the energy of a photon.

$$E = \hbar\omega = \frac{hc}{\lambda} \quad (1)$$

Where  $\hbar$  is the Planck constant divided by  $2\pi$ ,  $c$  speed of light,  $\omega$  frequency of the transition and  $\lambda$  wavelength of the transition. Usually, a common method to measure Stokes shift is taking into account the maximum peaks from absorption and fluorescence spectra (Figure 3).

$$\Delta\lambda = |\lambda^{max,flu} - \lambda^{max,abs}| \quad (2)$$

### 1.3 Frack-Condom Principle

Franck-Condon principle is a spectroscopy rule that explains the possible vibrational transitions. So, first of all, Born-Oppenheimer approximation give us a first approach of the energy. It says electrons move much faster than nuclei due to protons and neutrons are 1870 times more massive than electrons. Hence wavefunctions can be separated as follows.

$$\Phi(\vec{r}, \vec{R}) = \phi(\vec{r})_{electrons} \cdot \phi(\vec{r}(\vec{R}))_{nuclei} \quad (3)$$

Where  $\vec{r}$  is the electron coordinate while  $\vec{R}$  is the nuclear coordinate. In such case, only electronic contributions are considered in the Schrödinger equation. Once vibrational components are also included in the problem, vibrational-rotation states appear. As it is represented in Figure 2, vertical transitions between vibrational states ( $\nu \rightarrow \nu'$ ) can be obtained.

At the end, each electronic state contain vibrational states and the vibrational transitions are directly proportional to

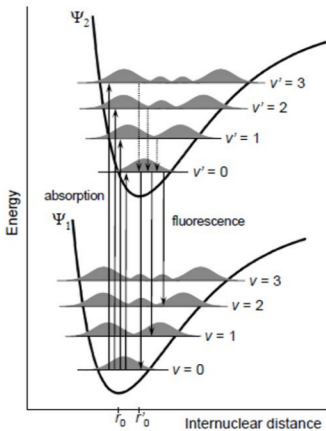


Figure 2: Vertical transitions between vibrational states. Source [2].

the overlap integral between the vibrational wavefunctions of the initial and final states.

$$P_{i \rightarrow f} = | \langle \psi_{final} | \vec{\mu} \cdot \vec{E} | \psi_{initial} \rangle |^2 \\ = | \int \psi_{final}^* (\vec{\mu} \cdot \vec{E}) \psi_{initial} d\vec{r} |^2 \quad (4)$$

This effect can be measured in terms of vibronic progression. Figure 3 shows clearly the effect of vibronic progression. In the left side absorption and fluorescence spectra is identified as a electronic transition while in the right side, vibrational transitions also appear in the spectra.

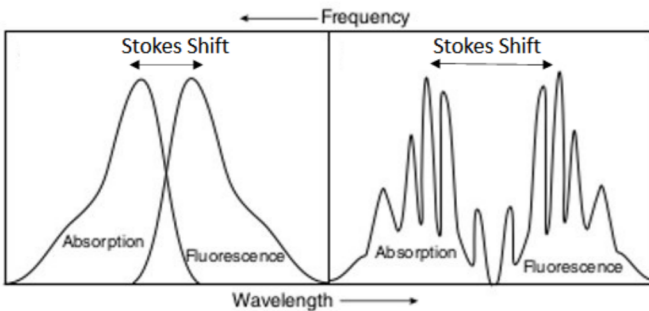


Figure 3: In the left, absorption and fluorescence spectra are shown. In the right, same picture but considering vibrational transitions. Source [2].

The Franck-Condon principle applied equally to fluorescence and absorption. So, it is important to note that excitation in higher energy states gives rise to fast intersystem crossing to lower state, until it reaches the first excited state and fluorescence occurs. This phenomenon is called as Kasha's rule [2].

## 1.4 Fluorophores

A fluorophore is chemical compound that can re-emit electromagnetic waves under the influence of light excitation.

Fluorophores generally include different combined aromatic groups, or planar or cyclic molecules with several  $\pi$  bonds.

Fluorophores display a characteristic sensitivity of emission parameters to their immediate environment. The fluorophores are chemical compounds which exhibit important distinctions in their electronic distribution, such as relative polarities, ground and first excited states. These variations allow the solvent molecules to interact with the ground and excited states in a different way, hence they change the energy gaps between these states.

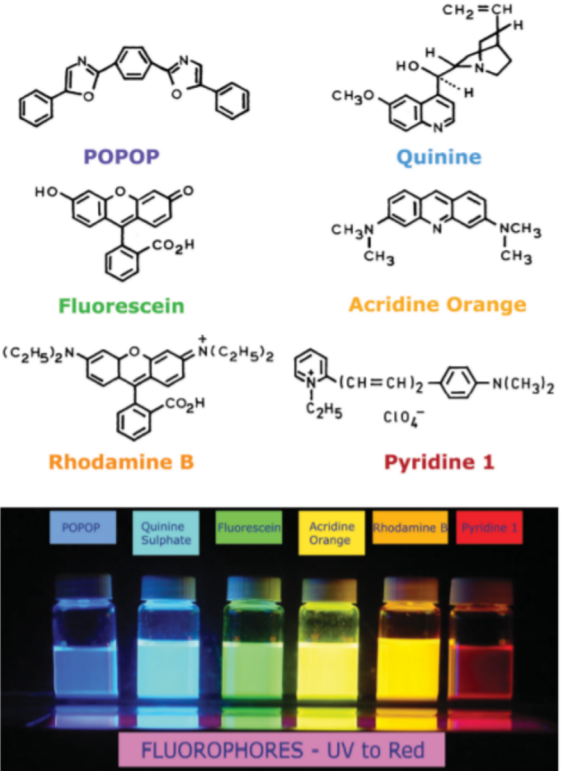


Figure 4: Structures of typical fluorescent substances [2].

## 1.5 Anisotropy

Fluorophores need an external excitation before the fluorescence process, such excitation can be done by an external polarized light. In an isotropic ensemble of molecules, transition dipole moment ( $\vec{\mu}$ ), that has a certain direction, would be randomly distributed. Hence polarization light will preferably excite molecules parallel/anti-parallel (or closely parallel/anti-parallel) than perpendicular dipole moments with respect to the applied electric field ( $\vec{E}$ ), as it is represented in equation (4) and figure 5.

In other words, it is a probabilistic process where transition dipole moment and applied electric field are the main ingredients. Since transition dipole moments are more likely to be excited if they are in a parallel (nearly parallel) direction of the applied polarization, then the excitations will occur unequally, it will be an anisotropy excitation in a photoselection

process. Anisotropy ( $\langle R \rangle$ ) can be measured as a combination of vertical-horizontal intensities.

$$\langle R \rangle = \frac{I_{VV} - G \times I_{VH}}{I_{VV} + 2G \times I_{VH}} \quad (5)$$

$$G = \frac{I_{HV}}{I_{HH}} \quad (6)$$

Where first index represents the orientation of excitation polarizer and second index represents the orientation of emission polarizer (Figure 5). Then, different intensity components are:

- $I_{VV}$ : Vertical component of the excitation polarizer and vertical component of the emission polarizer.
- $I_{VH}$ : Vertical component of the excitation polarizer and horizontal component of the emission polarizer.
- $I_{HV}$ : Horizontal component of the excitation polarizer and vertical component of the emission polarizer.
- $I_{HH}$ : Horizontal component of the excitation polarizer and Horizontal component of the emission polarizer.

Furthermore, one can already notice main important ingredients of equation (5) and (6), and its meanings. So, first of all, anisotropy equation measures the fluorescence process of a molecule upon different orientations in space. In more details, the fluorophore will be excited with different light polarization, vertical or horizontal, then the emission process will be different for vertical and horizontal excitations, such effect is captured and collected in equation (5). Furthermore, it is divided by a normalization factor, this factor comes from the isotropic distribution. Finally, anisotropy formula has the so called "G-factor", which is known as an error correction on anisotropy formula [3].

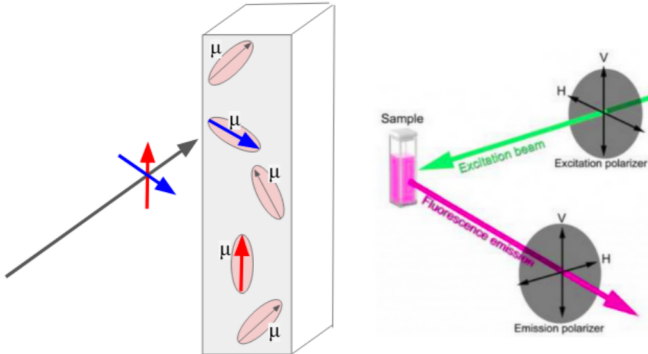


Figure 5: In the left, schematic diagram of polarization light orientation and a random ensemble of molecules with its transition dipole moment. In the right, a very simplified picture of the experimental setup (source [4]). Here, excitation polarizer and emission polarizer are shown.

## 1.6 Fluorescence quantum yield

However, fluorescence is not the unique process we can get in the an emission process, there are also some competing processes which can inhibit our fluorescence signal, most of them are expressed in the Jablonski diagram. The strength of the fluorescence is usually expressed by the fluorescence quantum yield ( $\phi_F$ ). It counts the amount of emitted photons versus the amount of absorbed photons. Then, the competing processes will relax the electrons in different pathways and fluorescence quantum yield will decrease.

$$\phi_F = \frac{k_F}{k_F + k_{nr}} \quad (7)$$

In other words, upon excitation fluorescence will occur but also electrons can leave the first excited state by other vias, those vias are non-radiative processes. We can highlight some of them as quenching processes, intersystem crossing, internal conversion...

## 1.7 Lifetime

An important concept in fluorescence is the lifetime. It is the time that takes until photons are emitted as a spontaneous emission. In ideal conditions, where there are not radiative-less processes, fluorescence lifetime is called natural lifetime.

$$\tau_F = \frac{1}{k_F} = \frac{1}{\Gamma} \quad (8)$$

However, if we take into account the non-radiative processes, we must modify equation 4.

$$\tau = \frac{1}{\Gamma + k_{nr}} = \phi_F \tau_F \quad (9)$$

Where  $\Gamma$  is the radiative decay rate. As we can see in equation 5, it can be used for the radiative lifetime calculation if we know the fluorescence quantum yield.

Lifetime of excited state represent the average time until electrons return to the ground state. However, during fluorescence emission process, a couple of conformation states can occur, then there is not any unique fluorescence lifetime will appear, there will be several lifetimes. In order to get a more tangible situation, if there are two conformation states, there would be two different lifetimes.

$$I(t) = \sum_i a_i e^{-t/\tau_i} \quad (10)$$

Where  $i$ -th component represent a characteristic fluorescence process. Here is expressed the main difference between steady state and time-resolved fluorescence experiment. Steady state measure an average over all  $i$ th-intensities decay of the fluorophore. It is usually performed by a constant illumination beam and the signal is recorded.

However time-resolved fluorescence experiments are performed by applying short pulses, typically these pulses are shorter than decay times and then intensity and anisotropy are recorded as a function of time. At the end, steady state experiment is the most common and simple one while time-resolved experiment is quite complex but it offers much more information about the fluorescence process.

## 1.8 Steady-state fluorescence

The emission of fluorescence can occur spontaneously because of transitions from electronic excited states. Fluorescence signal can be classified by various parameters such intensity, quantum yield, lifetime and polarization. In the steady-state method, radiation of the fluorescence due to spontaneous emissions are examined in comparably longer time period by tracking sample average. The method can be possible by intensity measurements related with emission wavelength.

Further, it should be mentioned that the interaction of fluorophores with their environment can affect the fluorescence parameters such as intensity, emission wavelength etc. The coupling with the environment is also depends on changing probability of relaxation processes or a new relaxation pathway.

## 1.9 Time-resolved fluorescence

Time-resolved fluorescence techniques are generally used to obtain emission lifetimes. Short exciting electromagnetic wave exposure upon sample, enable molecules to re-emit the response of short pulses. There are two different techniques considering the time-resolved fluorescence, pulse fluorimetry and phase-modulation fluorimetry. In pulse fluorimetry, short pulses are used to excite sample and the reactive emissions are measured. If we consider the phase-modulation fluorimetry, the modulated light is used with changing frequencies, thus creates the harmonic response of the sample. Therefore, it should be noted that first method works in the time domain, whereas, second one works in the frequency domain.

In contrast to steady-state method the fluorescence, there is not any spontaneous emissions measured in time-resolved emission spectra. Both techniques are frequently combined to observe time-resolved emission spectra(TRES).

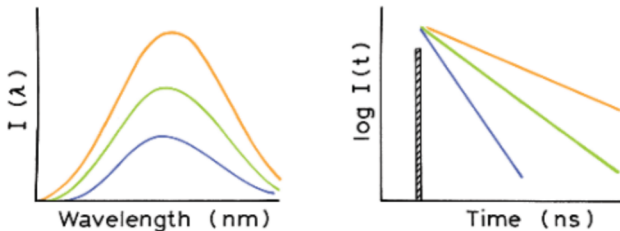


Figure 6: An example of steady-state fluorescence measurement (left) and time-resolved experiment (right). In the left, the experiment is performed by an average over all the fluorescence characteristics decays. In the right, short pulses of light are applied until intensity time dependence is captured [2].

## 2 Experimental procedure

The purpose of our experiment is to perform different fluorescence experiments for the lipid membrane. Then, we have performed steady states and time-resolved measurements.

Since our main goal is the study of the lipid membrane, we have also characterized the system with two samples.

**Vesicle Solution (Sample A):** It contains the lipid membranes, with the presence of the DMPC<sup>1</sup> molecules, and the dye, as DPH<sup>2</sup> molecule probe. Both molecules are diluted in water solution.

**Buffer Solution (Sample B):** It contains the dye, as DPH molecule probe, but is that case without the DMPC molecules, it is usually called "free dye". DPH is again diluted in water solution.

Figure 7 (top) shows an schematic picture of the vesicle and buffer solution. Additionally, Figure 7 (down) shows shape and view of vesicles and molecule probe

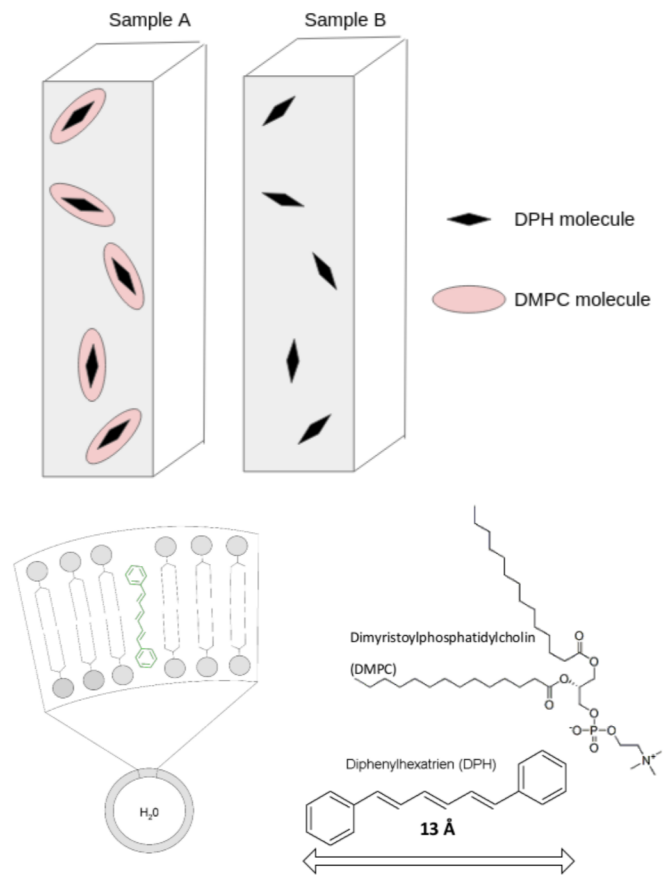


Figure 7: [Top] Vesicle -Sample A- and Buffer -Sample B- solutions are represented. Black symbols are the DPH molecule probes (dye) while pink circles are the DMPC molecules (vesicles). [Down] In the left, we have the lipid membrane, inside we have the DPH probe (right bottom) and the DMPC as a single sheets for the vesicle (right top). Source [5]

These samples are kept in cuvettes of  $4 \times 10 \text{ mm}$ . If one think about how it is possible to prepare  $100 \text{ ml}$  of  $1 \text{ mM}$

<sup>1</sup>The complete name for DMPC molecule is "Dimyristoylphosphatidylcholin".

<sup>2</sup>The complete name for DPH molecule is "Diphenylhexatriene".

DPH solution, we have to take into account the molar weight ( $M_w$ ) and formula of molarity.

$$\begin{aligned} M &= \frac{\text{mol}}{V} = \frac{\text{mass}}{M_w V} \rightarrow \text{mass} = M V M_w \\ &= 1 \times 10^{-3} (\text{mol/l}) \cdot 0.1 (\text{l}) \cdot 232.3 (\text{g/mol}) \\ &= 0.02323 \text{ g} \end{aligned} \quad (11)$$

Then, we have to use 23.23 mg of DPH solution. With such samples we were able to prove we have vesicles in the sample A, which is our main study goal. For steady state and time-resolved measurement, we have continued working only with sample A, there, the experiments were done at different temperatures in order to capture the dynamic of the phase transition of the vesicles.

## 2.1 Biological background. Lipid membranes in our experiment

Lipid membrane is a biological membrane that is composed by living cells. It is part of the organism and living beings use it in their systems [6]. It is composed by two layers with a hydrophobic core, where, in our case the layers are the vesicles (DMPC molecules). In figure 8, there is an image from a real biological membrane.

An example of its uses is the photosynthesis. This membrane is able to convert an incident light (i. e from the sun) into energy by creating a gradient of ions between the layers. In more details,  $CO_2$  is got from the air, it is split inside the membrane and an additional electron runs through it, then the gradient of ions is created and the photosynthesis process is done [6]. For such reason, this membrane is usually found in plants and it is usually called "phospholipid bilayer membrane".

The phase transition of it is around  $23^\circ C$ . Below to this temperature, the tails of the vesicles presented less movements (ordered state) than above the phase transitions (disordered state). For such reason different experiments at different temperatures are performed.

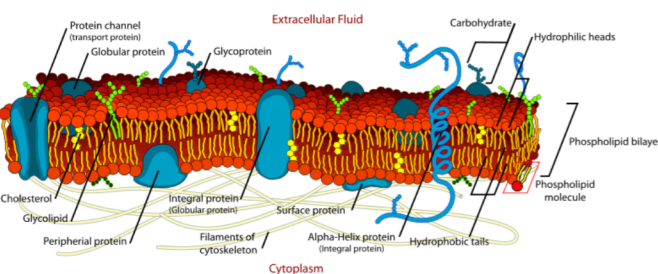


Figure 8: A real image of a biological membrane in an organism. As one can notice, others components of the living beings are represented. Then, complexes processes, as photosynthesis, can be performed with the combination of all components.

## 2.2 Experimental setup

We have collected some results from the steady-states at different temperatures, then we want to see how anisotropy depends on the temperature. Additionally we have applied time-resolved experiment by using a laser with the TCSPC method, then anisotropy can be measured in time. Experiment sketches are shown in figure 9.

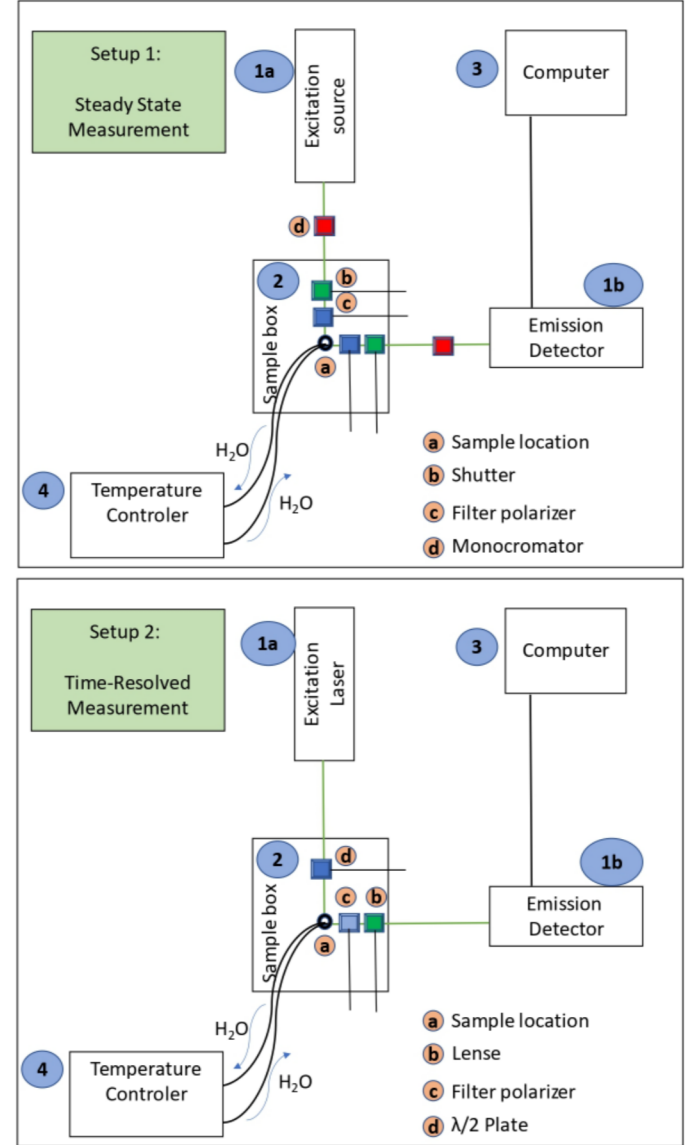


Figure 9: Steady-state (a) and time-resolved (b) experimental setup.

The experiments are composed by different devices, these devices are marked in the sketches. Regarding setup 1 (steady-state setup), first of all, (1a) represents the excitation source which is Xenon arc lamp. Further, (1b) represents the emission detector (also connected to PM1 in the laboratory). The light comes from the excitation source until it reaches the sample (2a), there, molecules are excited as it was explained in theory. In particular in "1.1 Introduction to Fluorescence and Absorption Processes" and "1.5

Anisotropy" sections. The wavelength of the excitation is varied by the monochromator (2d) and the polarization components are controlled by the filter polarizer (2c). Shutter device (2b) allows that light pass for a determined period of time, then it closes and opens for another measurement. All measures are recorded (and plotted) in the computer, then we saved the data for our own and future manipulations of it.

During this period of time, the absorption spectra was measured, the monochromator varied from  $\lambda_{ex}^{min} = 270 \text{ nm}$  to  $\lambda_{ex}^{max} = 420 \text{ nm}$  (with  $\lambda_{em} = 270 \text{ nm}$ ). Secondly, a fluorescence spectra was recorded. In such case the wavelength of the emission varied from  $\lambda_{em}^{min} = 380 \text{ nm}$  to  $\lambda_{em}^{max} = 530 \text{ nm}$  (with  $\lambda_{ex} = 360 \text{ nm}$ ). Fluorescence spectra was measured with sample A and sample B, in the same conditions, then, the objectives of these measurements were to obtain the characterization of both samples at the same time we get familiar with such apparatus. At that point, there are two important ingredients that still were not modified in the system:

- Temperature Controller (4) was not implemented yet, the measurements were done at room temperature.
- Intensity polarizer were not used yet.

Then, once we have characterized the system, we implemented the temperature controller and modified the intensity components with the filter polarizers. First of all, we measured the value of G-factor<sup>3</sup>. Due to it does not change under temperature it is only necessary to measure one time. For this task, we must implement the  $I_{HV}$  and  $I_{HH}$  configuration<sup>4</sup>, as it was explained in section "1.5 Anisotropy". Secondly we implemented the temperature controller, we changed to the  $I_{VV}$  and  $I_{VH}$  distribution and the anisotropy measurement is obtained at different temperatures. Temperatures went from  $T = 10 \text{ }^{\circ}\text{C}$  to  $T = 35 \text{ }^{\circ}\text{C}$ , close to  $T = 23 \text{ }^{\circ}\text{C}$  (phase transition), we used lower steps in order to get a more precise data.

Regarding to setup 2 (time-resolved measurement), the philosophy is almost the same. However, we used a laser for the excitation, in order to use the TCSPC method, which was already polarized (in the horizontal component). Again we measured all polarization components exposed in theory ( $I_{VV}$ ,  $I_{HV}$ ,  $I_{VH}$  and  $I_{HH}$ ), but in this case, at different time pulses and at three temperatures ( $T = 10.7 \text{ }^{\circ}\text{C}$ ,  $23.0 \text{ }^{\circ}\text{C}$ ,  $30.0 \text{ }^{\circ}\text{C}$ ). The anisotropy was recorded again but depending on time. Further explanations and results are discussed in the next section.

Setup 2 shows slightly different devices, first of all,  $\lambda/2$  plate (2d) was using to control the laser polarization. While a lens (2b) was implemented in the detector in order to not break it (due to the high power intensity of the laser). Furthermore, this experiment was not performed "instantaneously" as steady-state measurement. TCSPC takes some time until it reaches all the pulses to excite the photons. Each configuration took 3 minutes, then it was necessary to wait until 12 minutes in order to complete the experiment for one

<sup>3</sup>For this task, it is necessary to measure the zero voltage. It sets the zero reference in our detector PM2. Equation 15 shows explicitly how G-factor is affected

<sup>4</sup>Filters polarizers have sticks to turn on/off the horizontal or vertical component of the beam

temperature. During such time, temperature has to be stable, then some errors must occur due to fluctuations on it.

Finally it is important to remark that, although we used sample A for the measures, the response function of the system was also measured. Then we were able to see the scattering events that happen in sample B, which affect in short time decays for the intensity.

## 3 Results

### 3.1 Characterization of Fluorescence and Absorption

In our experiment, we must characterize the fluorophore probe, it is done with setup 1, which allows us to measure excitation and emission spectra at room temperature. Results are shown in Figure 10 and 11. Our results in clearly show Franck-Condon transitions in Figure 10, in particular there are four peaks. These peaks are reported in Table 1, as well as their oscillation frequencies.

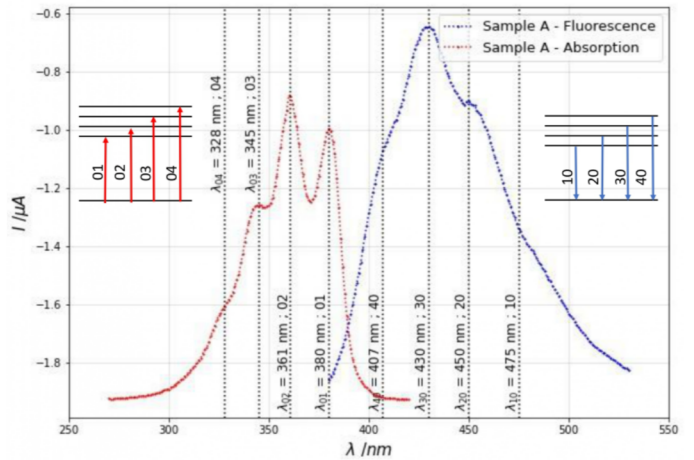


Figure 10: Absorption (red) and Fluorescence (blue) spectra for sample A. Peaks were recognized by using vertical lines and fitting it with the data. Furthermore, schematic energy diagrams have been done for each process.

The peaks were obtained using vertical lines in our data, then when the vertical line matches with the peak, then we obtained such value in the x-axis. For this task, as well as for the others, we used Python. In addition, our results show mirror shapes in both spectra and moreover we are able to identify the Stokes shift we have introduced in the theory section (equation 2). This result can be easily calculated by taking into account the difference of maximum peaks of each spectra.

$$\Delta\lambda = |\lambda_{j0} - \lambda_{02}| = 69 \text{ nm} \quad (12)$$

Once the sample A is characterize, we can procedure with sample B. As it has already been describe in *Experimental setup* section, it is mainly diluted in water, then we have a of quenching effects. Quenching effects are non-radiative processes, and hence measured intensity is much lower. Actually we have reduced the detector sensibility 100 order of

Vibrational level $\nu$	$\lambda_{\nu 0}(nm)$	$\omega_{\nu 0} (\times 10^{15} \text{ Hz})$
1	380	4.947
2	361	2.604
3	345	1.816
4	328	1.433
Vibrational level $\nu$	$\lambda_{0\nu}(nm)$	$\omega_{0\nu} (\times 10^{15} \text{ Hz})$
1	475	3.958
2	450	2.089
3	430	1.457
4	407	1.155

Table 1: Absorption and Fluorescence peaks are exposed. First of all, wavelength is recognized in Figure 10 and oscillation frequency is calculate for vibrational levels  $\nu$  (equation 1).

magnitude (from  $3 \mu\text{A}$  to  $3 n\text{A}$ ) in order to get a reasonable measurement. However, it is useful enough if we want to measure the ratio of emitted photons by sample A and sample B. In order to achieve this goal, we must to take into account all emitted photons in sample A and sample B, then we can get a ratio from quantum yields in both samples.

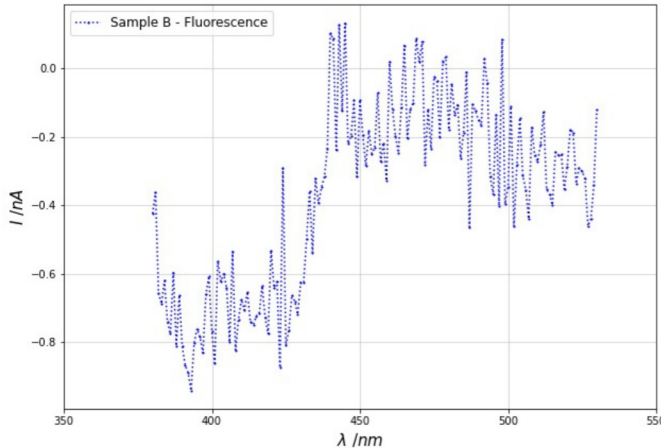


Figure 11: Fluorescence spectra for sample B. Measured intensity has been reduced due to the presence of quenchers.

$$\frac{\phi^B(k_r, k_{nr}, DPH_{H_2O})}{\phi^A(k_r, k_{nr}, DPH_{Lipid})} = \frac{N_B}{N_A} = \frac{-0.055833}{-193.598} = 0.000288 \quad (13)$$

Where  $N_A$  ( $N_B$ )<sup>5</sup> represents number of emitted photons by the sample A (sample B). There are other non-radiative processes but in principle the presence of water is the most important factor where quenchers come from. At the end, calculations lead up to obtain a ratio of 0.288. This value is totally since it give us a reasonable parameter for the quantum yield. One can modify it slightly and realize quantum yield

<sup>5</sup>In order to understand  $N_B$  and  $N_A$  better, it is useful if we write down an explicit formula for such calculations. Fluorescence spectra goes from 380 to 530, then our integration would be  $N_A = \int_{380\text{nm}}^{530\text{nm}} I^A(\nu, T) d\nu$  and  $N_B = \int_{380\text{nm}}^{530\text{nm}} I^B(\nu, T) d\nu$

of sample B has decreased and it is 4 times lower than for sample A.

$$\begin{aligned} \phi^B &= 0.288 \times 10^{-3} \quad \phi^A \approx \frac{1}{4} \times 10^{-3} \phi^A \\ &\longrightarrow \phi^A \approx 4000 \phi^B \end{aligned} \quad (14)$$

This fact is due to the quenching effects in the sample B. Moreover, absorption spectra for sample B is not needed because it does not affect into the excitations, hence it is equal to sample A.

### 3.2 Steady state

In this section, data from sample A measurements regarding different polarization configuration will be analyzed to calculate anisotropy as a function of temperature, then conversion yield with the help of fitting parameters of anisotropy over temperature curve, will be indicated. Thus, under favor of slope of the conversion yield over temperature van't Hoff enthalpy at melting temperature can become obtainable.

First, in order to determine the anisotropy values for our plots, G value is essential. Therefore, it is needed to perform a measurement with closed shutters as a reference measurement to take into account zero voltage of PMT which was obtained as  $I_0 = -1.3\mu\text{A}$ . Thus, G value can be obtained more accurately.

Afterwards, there are two different polarization configuration measurement should be implemented.  $I_{HV}$  which is a measurement of current obtained by arranging excitation polarizer to horizontal (pulled out) and the emission polarizer to vertical (pushed in), then emission polarizer was set to horizontal (pulled out) to measure  $I_{HH}$ . Thus, values for different polarization for emission  $I_{HV} = -0.7708\mu\text{A}$  and  $I_{HH} = -0.5377\mu\text{A}$  has been received. Merging  $G = I_{HV}/I_{HH}$  formula and zero voltage as in equation [15], G was calculated as  $G = 0.68 \pm 0.01$ , also for cross checking G value, it has been reported that the value, obtained from previous experiments, is highly close to  $G = 0.7$ , which indicates our G value is compatible with general results for our polarizers.

$$G = \frac{I_{HV} - I_0}{I_{HH} - I_0} = 0.68 \pm 0.01 \quad (15)$$

Where the errors from  $I_{HV}$  and  $I_{HH}$  were given by the software used in the laboratory. Then, error propagation was applied in order to obtain the G-factor. With the installation of refrigerant and thermometer, anisotropy measurements were started. Detection wavelength was set to 450nm and the orientation of the excitation polarizer has switched to vertical. During the measurement we consecutively switched the orientation of emission polarizer and measured the intensity for both vertically and horizontally polarized emissions. Moreover, we could obtain the uncertainties of the measurements from the computer software. In order to stabilize temperature of the sample, refrigerant set to certain temperatures step by step from around 10 degC to 35 degC. During the temporary stabilization for each temperature value PMT-voltage measured three to five times for switching the polarization configurations of emission polarizer. Anisotropy assessed by using equation (5) and our PMT voltage values.

$$R = \frac{I_{VV} - G \cdot I_{VH}}{I_{VV} + 2G \cdot I_{VH}} \quad (16)$$

Where R is anisotropy.

$$\sigma_R = \sqrt{\left(\frac{\partial R}{\partial I_{vv}}\sigma_{I_{vv}}\right)^2 + \left(\frac{\partial R}{\partial I_{vh}}\sigma_{I_{vh}}\right)^2 + \left(\frac{\partial R}{\partial G}\sigma_G\right)^2} \quad (17)$$

Where  $\sigma$  is used to define uncertainties of each parameter. Eventually, because our data is in reverse s shaped which indicates two steady states and fast exponential decrease in anisotropy within a short temperature interval because it shows phase transition. Sigmoid function seemed to be the best fit, then we used equation (18) to fit our data.

$$R(T) = \frac{A}{1 + \exp\left(\frac{T-T_m}{\tau}\right)} + m \cdot T + n \quad (18)$$

In this equation, A shows the step height,  $T_m$  is associated with the transition(melting) temperature and shows turning point of the curve.  $\tau$  defines the decay width, m and n indicate a linear baseline. These parameters are summarized in Table 2.

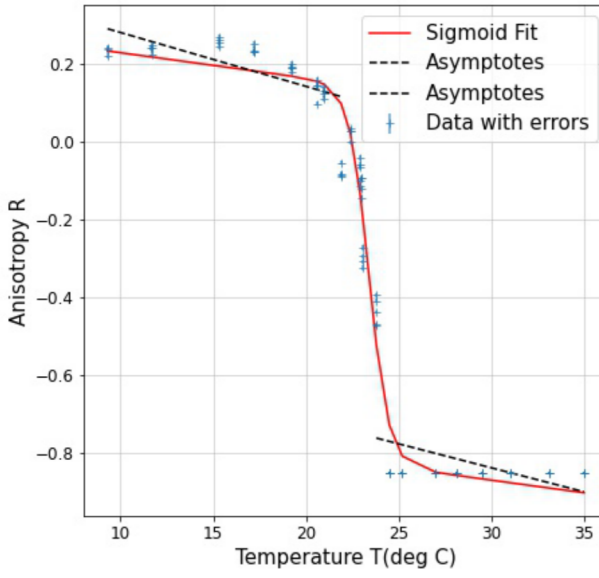


Figure 12: Anisotropy vs Temperature, exponential fitting applied to receive M1 and M2 values

Under favor of fitting parameters, the conversion yield of an equilibrium reaction arises from the transition of the lipid vesicle from gel-like phase to liquid crystal phase, can be calculated. Taking advantage of the distance between the upper and bottom asymptotes, which are obtained by using oblique asymptotes and arranged in equations (20),(21) considering the equation (19), one can obtain  $\Theta$  as a function of anisotropy, temperature and fitting parameters of sigmoid function as it is shown in equation (24).

Parameter	Value	Uncertainty
A	-0.970	$\pm 0.002$
$T_m(^{\circ}C)$	23.4	$\pm 0.1$
$\tau(^{\circ}C)$	0.527	$\pm 0.002$
$m (^{\circ}C^{-1})$	$-6.486 \cdot 10^{-3}$	$\pm 8 \cdot 10^{-6}$
n	0.293	$\pm 0.002$

Table 2: The parameters are belong to Figure 11 which sigmoid function used as a fitting method

$$\Theta = \frac{M_2}{M_2 + M_1} \quad (19)$$

[5]

$$M_1 = mT + n - R(T) \quad (20)$$

$$M_2 = R(T) - mT + n + A \quad (21)$$

$$\Theta = \frac{R - m \cdot T - n}{A} \quad (22)$$

Afterwards, with the calculated values of the conversion yield,  $\Theta$  vs temperature graph was plotted in the Figure 12. Further, their uncertainties again calculated with propagation of uncertainty method for independent variables even though the anisotropy is a function of temperature. Error propagation for dependent variable method was neglected because considering the magnitude of uncertainties there will not be any significant change. It could give relatively smaller uncertainties as in previous graph Figure 12.

$$\sigma_{\Theta} = \sqrt{\left(\frac{\partial \Theta}{\partial R}\right)^2 \sigma_R^2 + \left(\frac{\partial \Theta}{\partial T}\right)^2 \sigma_T^2 + \left(\frac{\partial \Theta}{\partial m}\right)^2 \sigma_m^2 + \left(\frac{\partial \Theta}{\partial n}\right)^2 \sigma_n^2 + \left(\frac{\partial \Theta}{\partial A}\right)^2 \sigma_A^2} \quad (23)$$

Because of theta vs temperature graph's form, again we could fit without baseline parameters since it start from zero and its parameters which hold with previous fit are given in table below.

$$\Theta(T) = \frac{1}{1 + \exp\left(\frac{-(T-T_m)}{\tau_m}\right)} \quad (24)$$

Parameter	Value	Uncertainty
$T_m(^{\circ}C)$	23.4	$\pm 0.1$
$\tau(^{\circ}C)$	0.527	$\pm 0.002$

Table 3: Melting temperature and decaying constant obtained by parameters of the linear fit in conversion yield vs temperature plot

$\chi = 0.599$  is the chi square value of the Linear Regression Fit and it is indeed small, thus it can be said that linear fit is significantly successful to apply for conversion yield data.

The function  $\Theta(T)$  can be interpreted by an equilibrium reaction between  $M_1$ (lower asymptote) and  $M_2$ (upper asymptote) with equilibrium constant such as:

$$k = \frac{M_2}{M_1} = k_0 \exp \frac{\delta H}{4R'^2} \quad (25)$$

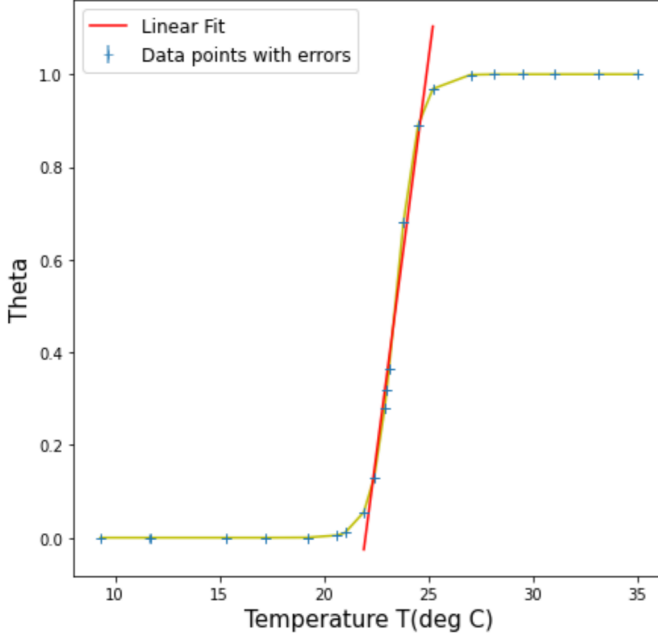


Figure 13: Conversion yield of an equilibrium reaction(Theta) over temperature plot, Linear regression applied as a fitting method.

Where R' is molar gas constant. Considering equations (19), (20), (21) one simple thing is that the slope of linear fit in  $\Theta(T)$  vs temperature plot in Figure 13 can be used to calculate enthalpy of the phase transition with the help of relation between chemical equilibrium constants and enthalpy change. This brilliant relation is called van't Hoff enthalpy and it has been generally useful to examine the changes in state functions for thermodynamic systems. Hence, deriving the equations (26) and (27) and the slope of the fit shown in Figure 13, used in equations (26) and (27) to reach the ratio of enthalpy change over temperature.

$$\frac{\partial \Theta}{\partial T} \Big|_{T=T_m} = \frac{\delta H}{4R' \cdot T^2} \quad (26)$$

$$\delta H = 4R' \cdot T^2 \cdot \frac{\partial \Theta}{\partial T} \Big|_{T=T_m} \quad (27)$$

From Ref. [5], our van't Hoff enthalpy value becomes available as,

$$\delta H = 4368 \pm 116 \frac{kJ}{mol} \quad (28)$$

Again, its level of confidence has been calculated by gaussian error propagation.

$$\sigma_{\delta H} = \sqrt{\left(8R'T \cdot \frac{\partial \Theta}{\partial T} \Big|_{T=T_m} \cdot \sigma_T\right)^2 + (4R'T^2 \cdot \sigma_{\frac{\partial \Theta}{\partial T}} \Big|_{T=T_m})^2} \quad (29)$$

### 3.3 Time-resolved fluorescence

Another technique for measuring anisotropy is time resolved spectroscopy. The data obtained using the time resolved ap-

proach is in the form of lifetimes, from which perpendicular and parallel intensities can be calculated. To ensure that the equipment is functioning properly, we must first measure the response function of the instrument. The Instrument response function(IRF) give us the timing precision to the overall time-correlated single photon counting(TCSPC) system. If we have accurate detectors, sharp excitation pulse and electronics then we will see very narrow IRF which means system is ideal. If we see any deviation in the peak of IRF then it might be source of instrumental error. The response function of the data can be measured using a sample as saturated water with DPH in THF, and then using the Becker and Hickel software on a computer to generate a graph of the number of counts vs time. Figure 14 depicts the equipment response function. The buffer solution gives us the response to setup. To get the response, the alignment of polarizer filter and laser must be vertical.

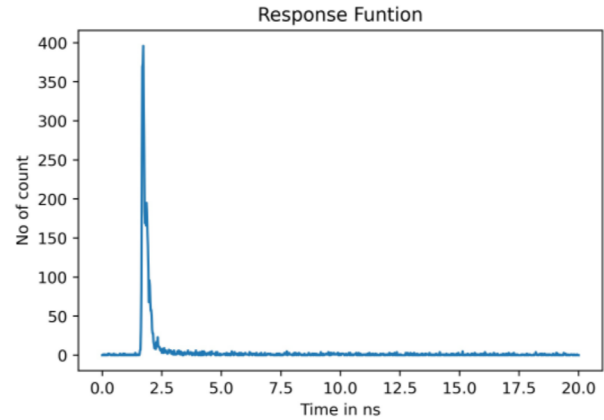


Figure 14: The instrument's response function without the use of a polarizer filter i.e vertically aligned, giving us a unfiltered laser pulse.

Now to obtain fluorescence signal we have to put vesicle sample into the setup. We have taken data at three different temperatures: 10.7°C, 23.0°C, and 30.0°C and for each temperature we obtained four lifetime decay curves. Each curve represents the polarizer filter's orientation. The software Becker and Hickel give the data points in terms of block or page so for four curves we have four page which corresponds to the position of filters. The laser for our first page is horizontally polarized, and the filter is also horizontal. With the filter and laser oriented to only pass horizontal polarization of light, we get the intensity of our first curve. By adjusting the position of the filter and laser and repeating the operation, which takes around 180 seconds, we can see all four intensity curves in the software.

To determine time-resolved anisotropy G-factor is required. The G factor is obtained using equation (17) and the values of  $I_{hv}, I_{hh}$  at each point, then the average of the G factor points is calculated. The G-factors for 10.7°C, 23.0°C, and 30.0°C were roughly 1.01, 0.71, and 0.95, respectively.

Equation (16) is used to calculate the value of anisotropy. We require the intensity of all curves at each point ( $I_{vv}$ ,  $I_{vh}$ ,  $I_{hv}$ , and  $I_{hh}$ ) to calculate anisotropy. Figure 18 shows the

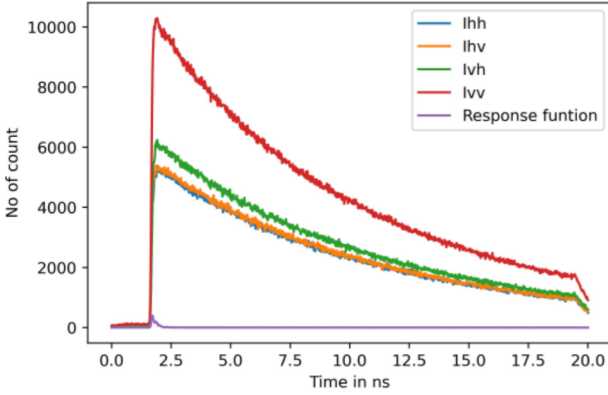


Figure 15: Intensity curve for all possible alignment of the polarizer at 10.7°C.

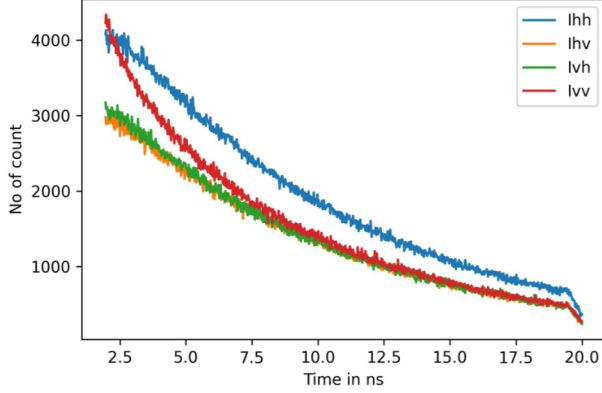


Figure 16: Intensity curve for all possible alignment of the polarizer at 23.0°C.

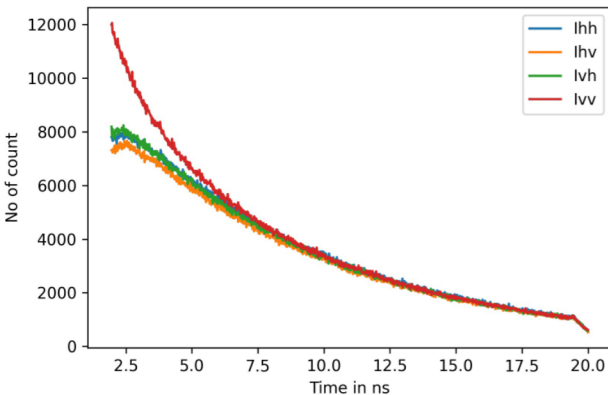


Figure 17: Intensity curve for all possible alignment of the polarizer at 30.0°C.

anisotropy of 10.7°C, 23.0°C, and 30°C, indicating the phase transition of the sample from solid to liquid.

Our anisotropy value came from figure 18. Table 4 shows the calculated value of Anisotropy( $\langle R \rangle$ ) as well as the corresponding temperature. To come at our result, we average each anisotropy points at the each temperature.

Temperature	$\langle R \rangle$
10.7°C	0.15
23.0°C	0.11
30.0°C	0.03

Table 4: Average value of anisotropy at measured temperature.

The fluorescence anisotropy decay is analysed by

$$r(t) = (r_0 - r_\infty) \exp \frac{-t}{\phi} + r_\infty \quad (30)$$

where  $r_0$  is fundamental anisotropy,  $r_\infty$  is residual anisotropy and  $\phi$  is correlation time.

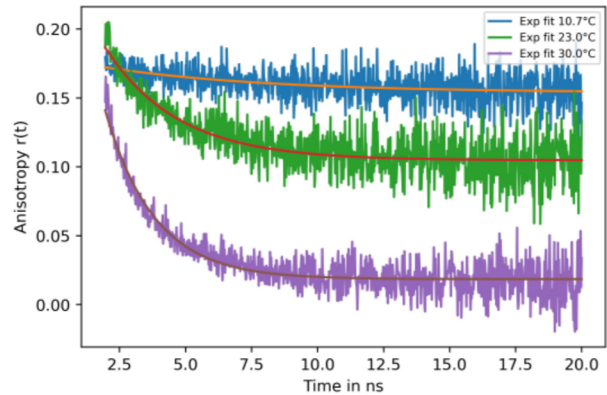


Figure 18: Exponential fit of fluorescence anisotropy decay at 10.7°C, 23.0°C and 30°C.

From fluorescence anisotropy decay curve we got:  
For 10.7°C,

$$r(t) = (0.02) \exp \frac{-t}{6.24} + 0.15 \quad (31)$$

For 23.0°C,

$$r(t) = (0.16) \exp \frac{-t}{2.74} + 0.10 \quad (32)$$

For 30.0°C,

$$r(t) = (0.35) \exp \frac{-t}{1.85} + 0.01 \quad (33)$$

The Micro-viscosity is related with the apparent relaxation time  $\phi$ , which is given by

$$\phi = \frac{1}{6D} \quad (34)$$

where, D is the orientational diffusion coefficient [7]. The viscosity of lipid membrane is probably one of the most important factor for understanding the dynamics of cell membrane.

Hence, in order to calculate the micro viscosity of molecule we used the Debye-Stokes-Einstens relation. [8].

$$\eta = \frac{KT}{6D\mu_h} \quad (35)$$

To measure the rotation of our DPH probe, we also calculated the angle between the normal of lipid membrane and the DPH probe. Also called as the wobbling-in-cone angle. [9], For this we need  $r_\infty$  and  $r_0$

$$(r_\infty/r_0) = \sqrt{1/2 \cdot \cos\theta(1 + \cos\theta)} \quad (36)$$

Parameters	10.7°C	23.0°C	30.0°C
$\phi(ns)$	6.24	2.74	1.85
$\eta(Pa.ms)$	5.65	5.33	4.70
$\theta(degree)$	79.63	83.05	70.42
$\tau(ns)^{-1}$	8.81	6.48	5.67

Table 5: All the calculated parameters from the anisotropy curve.

## 4 Conclusions

In our experiment we were able to measure two samples. Sample A was the vesicle solution, where we find the lipid membrane and the DPH molecule probe diluted in water, while sample B was buffer solution, where we do not have the lipid membrane anymore. We were able to characterize both systems with absorption and fluorescence spectra, then we realized there are quite more quenching effects in sample B than in sample A, as we expected. Although fluorescence spectra for sample B got some noise, we were able to even calculate this amount of quenchers which the ratio of quantum yield A and B.

At the end, we got a 4000 times higher quantum yield for sample A, which represent less quenching effects in the sample. However, this results must be around 200, instead of 4000, it can be justified due to impurities in the samples, especially in sample B. Then even more quenching effects can appear. Actually a little contamination of samples can highly change the results of the quantum yield. Moreover, an important note is that we did not do the absorption spectra from sample B because it will not be affected by the quenching, then absorption spectra can only be measured one time.

Furthermore, vibration levels were identified for absorption and fluorescence spectra. Vibration progressions of Franck-Condon transitions were captured and a mirror shape was obtained as it was expected from the theory part. Then, Stokes shift was also calculated by taking the maximum peaks for absorption and fluorescence spectra, around 69 nm in our case. Finally and more important about this characterization. We were able to really prove that sample A has vesicles in the system, then we could continue working with this sample and study the lipid membrane more in deep with steady states and time-resolved fluorescence measurements.

In steady state part, we only examined the data which measured by arranging different configurations for polarization

from sample A, because it includes concentration of vesicles. Anisotropy measurement was done by measuring emission intensities via PMT-voltage devices. After we calculated our G value as a ratio of HV and HH orientations previously mentioned for steady state emission measurements. Afterwards, anisotropy calculations were done by fitting sigmoid function on anisotropy vs temperature data. Finally, for anisotropy and  $\theta$  curves we implemented sigmoid function as a best choice. The melting temperature estimated by one of the fitting parameters highly close to real phase transition temperature, in our case we were able to measure the phase transition temperature as  $T = 23.40^\circ C$  which is quite close to  $T = 23.00^\circ C$ . Thus, we could conclude our measurement was done successfully. Further, this means that our sample had been prepared carefully and impurities may affect the hydrophobic environment created by DMPC, were able to be avoided. Hence, during phase transition our sample was homogeneously heated by the temperature controller.

With the help of parameters obtained from sigmoid function, conversion yield of an equilibrium reaction could be demonstrated as a function of temperature and anisotropy. Further, slope of this function used to calculate van't Hoff enthalpy, the value is way more higher than calorimetric measurement as we expected. In our case enthalpy was measured  $\delta H = 4368 \frac{kJ}{mol}$  while the calorimetric measurement is  $\delta H = 30 \frac{kJ}{mol}$ . This fact can be explained by couple of reasons. For instance, van der Waals forces lead the alignment of the neighbouring organic chains in particularly if the organic chains are longer. Hence, though vesicle molecules reach the phase transition some of the chains cannot have enough freedom. Thus, we can conclude that gel-like areas in the vesicle membrane may become attached to the other chains which results sharp phase transition corresponding to large van't Hoff enthalpy.

For the t resolved anisotropy method, we take measurement at three different temperature; 10.7°C, 23.0°C, and 30.0°C. After calculating the G factor we saw change in our G factor at different temperature. we got 1.01, 0.71, and 0.95, respectively. In principle, G factor should not change under the influence of the time. However, we can clearly see that there are some differences, specially at the phase transition. The other two values are in agreement each other so this main difference of the G value comes due to the fact in the main transition and fluctuations becomes bigger. Also, temperature fluctuation can be reason for the change of G factor. Furthermore, from the G factor and intensity of all curve we got our average anisotropy around 0.15, 0.11 and 0.03 for corresponding temperature. When we compare the results to the steady-state, we can see that the values of anisotropy for 10.7°C and 23.0°C are practically same, but for 30.0°C, there is a significant difference. This difference could be caused by a variety of factors. Sometimes we saw temperature fluctuates while being measured. We also cannot overlook the instrument's response function. Again, change in G-factor could also be the reason behind the variation of anisotropy. Also, while taking measurement of steady state our photometer got over loaded.

From the exponential fit of anisotropy curve, we got all of our required parameters which are mentioned table 5. From

the parameter such as Viscosity, wobbling cone angle, we can analyse the influence of DPH probe over the lipid membrane. As expected, the decreasing value of these parameters with increasing temperature shows us the phase transition of our molecule.

## 5 Appendix

### 5.1 Error propagation

Error propagation for anisotropy

$$\begin{aligned}\sigma_R &= \sqrt{\left(\frac{\partial R}{\partial I_{vv}}\sigma_{I_{vv}}\right)^2 + \left(\frac{\partial R}{\partial I_{vh}}\sigma_{I_{vh}}\right)^2 + \left(\frac{\partial R}{\partial G}\sigma_G\right)^2} \\ &= \sqrt{P_1^2 + P_2^2 + P_3^2}\end{aligned}\quad (37)$$

Where  $P_1$ ,  $P_2$  and  $P_3$  are:

$$\begin{aligned}P_1 &= \frac{\partial r}{\partial I_{vv}}\sigma_{I_{vv}} \\ &= \frac{1 \cdot (I_{vv} + 2 \cdot I_{vh}) - (I_{vv} - G \cdot I_{vh})}{(I_{vv} + 2 \cdot I_{vh})^2}\sigma_{I_{vv}}\end{aligned}\quad (38)$$

$$\begin{aligned}P_2 &= \frac{\partial r}{\partial I_{vh}}\sigma_{I_{vh}} \\ &= \frac{-G \cdot (I_{vv} + 2 \cdot I_{vh}) - 2 \cdot (I_{vv} - G \cdot I_{vh})}{(I_{vv} + 2 \cdot I_{vh})^2}\sigma_{I_{vh}}\end{aligned}\quad (39)$$

$$P_3 = \frac{\partial r}{\partial G}\sigma_G = -\frac{I_{vh}}{I_{vv} + 2 \cdot I_{vh}}\sigma_G \quad (40)$$

### 5.2 Python codes

```
#libraries
from sklearn import linear_model
import numpy as np
import pandas as pd
import matplotlib.pyplot as plt
from scipy.optimize import curve_fit
from sklearn.metrics import mean_squared_error

Error propagation for anisotropy

def error(Ivv, Ivh, AI_vv, AI_vh, G, AG):
    P1 = (((Ivv + 2*Ivh) - (Ivv - G*Ivh)) / (Ivv + 2*Ivh))*AI_vv
    P2 = ((-G*((Ivv + 2*Ivh) - 2*(Ivv - G*Ivh)) / (Ivv + 2*Ivh))*AI_vh
    P3 = -(Ivh*AG) / (Ivv + 2*Ivh))

    Ar = np.sqrt(P1**2 + P2**2 + P3**2)
    return Ar
```

Fitting with sigmoid function

```
def sigmoid(x, A, Tm, t, m, n):
    y = (A / (1 + np.exp(-(x-Tm)/t))) + m*x + n
    return (y)

p0 = [max(ani), np.median(temp), 1, 1, min(ani)]
which is a mandatory initial guess

popt, pcov = $curve_fit$(sigmoid, temp, ani, p0, method="dogbox")
```

Fitting with exponential function and calculating residuals

```
def nExp(t, fi, m, R_inf):
    return m * np.exp(-t / fi) + R_inf
```

Initial guess

```
p0 = [max(dt1), np.median(dt), min(dt1)]
```

```
popt, pcov = curve_fit(nExp, dt, dt1, p0, method="dogbox")
```

Calling parameters of fit

```
fi = popt[0]
m = popt[1]
R_inf = popt[2]
```

Calculating residuals

```
residuals = dt1 - nExp(dt, fi, m, R_inf)
fres = sum((residuals**2)/nExp(dt, fi, m, R_inf))
Which is for the chi-sqaure of our fit
```

## 6 References

- [1] Alexander Kyrychenko. Using fluorescence for studies of biological membranes: a review. 3(4):042003, oct 2015.
- [2] Joseph R. Lakowicz, editor. *Principles of Fluorescence Spectroscopy*. Springer US, 2006.
- [3] HORIBA Techonology. Fluorescence anisotropy studies. (Ref. Adapted from [1], <https://www.horiba.com/ind/technology/spectroscopy/fluorescence-spectroscopy/what-is-fluorescence-anisotropy-or-fluorescence-polarization/>).
- [4] HORIBA Techonology. Fluorescence anisotropy studies. (Ref. Adapted from [1]).
- [5] Manual from advanced laboratory course. ma 5: Dynamic processes in lipid membranes. (Ref. Adapted from [1]), 2021.

- [6] Wikipedia. Lipid bilayer. (Ref. Adapted from [1][https://en.wikipedia.org/wiki/Lipid<sub>b</sub>ilayer](https://en.wikipedia.org/wiki/Lipid_bilayer)).
- [7] Guoqing Jia, Zhaochi Feng, Chunying Wei, Jun Zhou, Xiuli Wang, and Can Li. Dynamic insight into the interaction between porphyrin and g-quadruplex dnas: Time-resolved fluorescence anisotropy study. *The Journal of Physical Chemistry B*, 113(50):16237–16245, 2009. PMID: 19924868.
- [8] Sumita Roy, Ashok Mohanty, and Joykrishna Dey. Microviscosity of bilayer membranes of some n-acylamino acid surfactants determined by fluorescence probe method. *Chemical Physics Letters*, 414:23–27, 2005.
- [9] Kazuhiko Kinosita, Akira Ikegami, and S Kawato. On the wobbling-in-cone analysis of fluorescence anisotropy decay. *Biophysical journal*, 37 2:461–4, 1982.